PROC. OF JSCE,
No. 280, DEC. 1978

BEARING CAPACITY OF INHOMOGENEOUS GROUND DETERMINED BY GRAPHICAL SOLUTION OF POLE TRAIL METHOD

By Koichi AKAI, Yuzo OHNISHI** and Hiroaki MIZOBE****

1. INTRODUCTION

Up to now in the case of stability analysis, it is often assumed that the soil medium has a uniform strength. Such an assumption gives satisfactory results for structures of moderate scale. For example, the well-known Terzaghi's equation of the bearing capacity seems to be derived from the fact that the size of footing was at most 20 feet (about 7 m) at his time.

However, in recent years, the foundations of structures are becoming larger and larger, and it is now necessary to examine the usefulness and the limit of the conventional stability analyses in order to estimate the stability of these structures.

When the stability analyses in soil mechanics and foundation engineering are carried out, it is known that the slip circle or slip line usually passes through the points of various depth. Therefore the assumption that the soil medium has a uniform strength, *e.g.* the cohesive strength c_u=constant (friction angle $\phi_u=0$) in the total stress analysis, may cause a large error especially for a large foundation whose influence range is very wide and deep. As a matter of fact, Taylor's table which was made with the assumption that c and ϕ are constant is not used in the stability analysis of slope (total stress analyses), but the calculation is usually performed by the method of slices with shear stress contour on the cross section of slope. The Terzaghi's equation of bearing capacity is analogous to the Taylor's table and seems to be applicable only for the idealized ground model, and the more realistic assumption has to be introduced in the analysis of bearing capacity. Therefore a new method of stability analysis is desired in order to examine the problem of inhomogeneity of strength, particularly the cohesive strength c_u is a function of depth from the ground surface in the total stress analysis.

Davis and Booker[1),2)] have developed a numerical solution of bearing capacity when the cohesive strength increases linearly with depth. Spencer[3)] also has presented an analytical perturbation method to the problem of an inhomogeneous ground, but his solution technique is applicable only to the case that the strength change is small enough to be perturbed. The purposes of this paper are to develop a new graphical method of the pole trail derived from the theory of plasticity, which is applicable to the case of inhomogeneity of strength, and to discuss the results of the application of the method to the foundation on the weathered granite rock mass. The results of the conventional stability analyses are also shown and compared with those of the graphical ones.

2. EQUATIONS OF BEARING CAPACITY

Along with the analysis of settlement which is made to ascertain that the foundation can fulfill their intended functions, the computation of ultimate loads is the fundamental work for the design of foundations.

The Terzaghi's equation of bearing capacity is still in common use for estimating the ultimate bearing capacity of foundations. This equation is derived from the load intensity at which the ground is just in the plastic state with active, radial shear and passive zones. The approximate value of the bearing capacity for a shallow foundation is given by the equation

$$q_d=cN_c+\frac{1}{2}\gamma BN_\gamma+\gamma D_fN_q \quad \cdots\cdots\cdots\cdots(1)$$

* Dr. Eng., Professor, Department of Transportation Engineering, Kyoto University.
** Ph. D., Associate Professor, Department of Transportation Engineering, Kyoto University.
*** Engineer, Tokyo Metropolitan City.

in which q_d is the ultimate bearing capacity, γ is the unit weight of soil, B is the width of foundation, D_f is the depth of foundation and the bearing capacity factors, N_c, N_γ, N_q are dimensionless quantities depending only on ϕ. These bearing capacity factors are formulized and tabulated for practical use considering the effect of the gravity weight and particularly for the sandy soil their values are easily estimated in relation to the N-value of the standard penetration test. The Terzaghi's equation of bearing capacity is useful for the various types of foundation and various depth of footing but it can not take into account the inhomogeneity such that the unit weight or strength parameters change in the ground.

The slip circle method to determine the bearing capacity of foundation is well-known as the Tschebotarioff-Wilson method. Tschebotarioff assumed that the slip failure of a continuous footing on the cohesive soil might occur along the cylindrical surfaces as shown in **Fig. 1** and the axis of rotation coincide with the edge of strip load, b. From the balance of rotational moment with respect to the point b at the instance of failure, the following bearing capacity is derived.

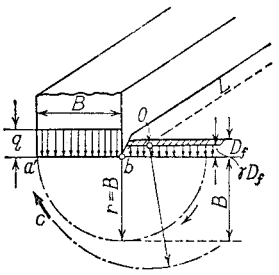

Fig. 1 Failure of Ground.

$$q_d=6.28c\left(1+0.32D_f/B+0.16\frac{\gamma}{c}D_f\right) \quad \cdots\cdots(2)$$

And also in the case that the bottom of the foundation is the ground surface ($D_f=0$),

$$q_d=6.28c \quad \cdots\cdots(3)$$

This value is a little bit larger than the following Prandtl solution which is based on the theory of plasticity.

$$q_d=5.14c \quad \cdots\cdots(4)$$

According to Terzaghi, this equation is valid only to the problem of foundation with a perfectly smooth base. In the case of a rough base, accounting for the restraining effect on the soil medium,

$$q_d=5.7c \quad \cdots\cdots(5)$$

Fellenius pointed out that the most critical position of the axis of rotation is not the point b and the bearing capacity as follows:

$$q_d=5.52c \quad \cdots\cdots(6)$$

Wilson calculated the position of the axis of rotation for the foundation with depth, D_f and obtained the equation:

$$q_d=5.52c(1+0.377D_f/B) \quad \cdots\cdots(7)$$

As is known from the above discussion, in the stability analyses there are two methods; the one is based on the theory of plasticity and the other is the slip circle method, which gives rise to the solution in the problems of bearing capacity of foundation on the ground surface and the critical height of excavated slope. However, the bearing capacity of the homogeneous ground determined by the slip circle method ($\phi=0$-analysis) is at most 8% greater than the lower bound solution by the theory of plasticity as is shown from the comparison between Eqs. (4) and (6).

Meanwhile, if the ground is assumed to be inhomogeneous the slip circle method estimates much larger value than the plasticity solution, whereas the analytical solution can be obtained only for the rather simple inhomogeneity such that the shear strength increases linearly with depth. For example, **Fig. 2** illustrates the comparison of the results of analyses[1),2)] by both methods for the problem, in which the undrained shear strength at the surface is c_0 and increases linearly with depth. It is known that the slip circle method very seriously overestimates bearing capacity when the increase of strength with detph is dominant.

The poor performance of the slip circle method can be understood when it is recognized that an adequate slip circle which sufficiently coincides with the trajectory of the velocity field can not

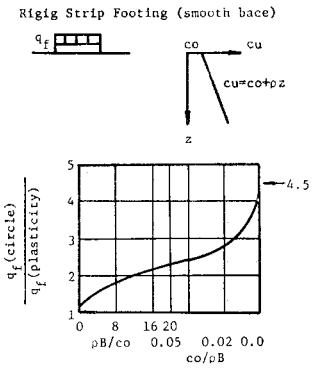

Fig. 2 Error in Slip Circle Analysis (after Davis and Booker).

be drawn in this method.

The correct critical slip line must satisfy, in the slip circle method or the slip non-circular method, that its safety factor is nearly equal to 1 and the shape of the slip line is similar to that of the actual failure. Therefore the problems of slope stability and bearing capacity of a foundation are essentially same, as the slip failure of ground is considered.

3. GRAPHICAL SOLUTION OF PLASTIC EQUILIBRIUM

(1) Introduction

It is extremely difficult to obtain the analytical solution of bearing capacity when a large scale foundation of a structure is on the inhomogeneous ground. However, the use of the graphical method of plastic equilibrium is often very effective. In this method, when the stress state of the close two points in the ground at the plastic equilibrium is known, that of the neighbouring third point can be determined tracing the slip lines in the physical space and the poles in the stress space. At the same time, the stress circle at failure is drawn by the pole method for each point of the slip lines which has a different magnitude of failure strength depending upon the inhomogeneity of the ground. With this method the bearing capacity of a foundation can be obtained for the inhomogeneous ground whose strength is not uniform.[5),6)]

(2) Equations for the Pole Trails (When the undrained shear strength c_u increases with depth)

The two-dimensional equations of equilibrium in stress state are always satisfied:

$$\left.\begin{aligned}\frac{\partial\sigma_x}{\partial x}+\frac{\partial\tau_{xz}}{\partial z}&=0\\ \frac{\partial\tau_{xz}}{\partial x}+\frac{\partial\sigma_z}{\partial z}&=\gamma\end{aligned}\right\} \quad \cdots\cdots(8)$$

where the Z-axis is assumed to be vertical with the positive direction downward. Here, the unit weight, γ is taken to be the body force only. The failure criterion of a purely cohesive soil is given by

$$\tau=c_u(z) \quad \cdots\cdots(9)$$

In **Fig. 3** (b), the Mohr circle represents the stress condition of an infinitesimal soil element shown in **Fig. 3** (a) and the major principal stress σ_1 of the element is assumed to be directed at an angle of θ to the Z-axis.

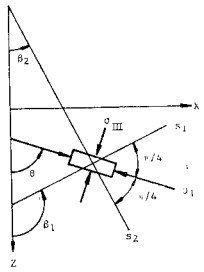

Fig. 3 (a)
Physical Space.

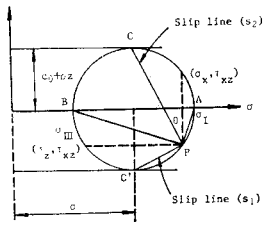

Fig. 3 (b)
Stress Space.

From the position of the pole of the element shown in **Fig. 3** (b), the directions of two slip lines can be found to be parallel to the straight lines passing through the pole P and points C, C′, the points of tangency of the circle of stress with the failure lines. These slip lines, PC and PC′, make equal angle $\pm\pi/4$ with the direction PB of the major principal stress in **Fig. 3** (b). The slip lines s_1 and s_2 in the physical space (**Fig. 3** (a)) are drawn parallel to the lines PC′ and PC. The angles β_1 and β_2 at which the slip lines of the element intersect with the Z-axis are

$$\left.\begin{aligned}\beta_1&=\theta+\pi/4\\ \beta_2&=\theta-\pi/4\end{aligned}\right\} \quad \cdots\cdots(10)$$

Let us now define a new variable, mean stress σ, where

$$\sigma=\frac{1}{2}(\sigma_x+\sigma_z)=\frac{1}{2}(\sigma_1+\sigma_{III}) \quad \cdots\cdots(11)$$

In **Fig. 3** (b), σ is represented by the center of the Mohr circle. Then expressing σ_x, σ_z and τ_{xz} at yield in terms of the two variables σ and θ, and substituting into Eq. (8), the following fundamental equations giving the variation in stress state along the slip lines are obtained:

along an s_1 line,

$$\frac{\partial\sigma}{\partial s_1}+2c_u(z)\frac{\partial\theta}{\partial s_1}=\gamma\cos\beta_1-\tan\beta_1\frac{\partial c_u(z)}{\partial s_1} \quad \cdots\cdots(12\cdot a)$$

along an s_2 line,

$$\frac{\partial\sigma}{\partial s_2}+2c_u(z)\frac{\partial\theta}{\partial s_2}=\gamma\cos\beta_2+\tan\beta_2\frac{\partial c_u(z)}{\partial s_2} \quad \cdots\cdots(12\cdot b)$$

The stress conditions in a state of plastic equilibrium and the directions of the two slip lines can be found from the position of the pole.

The position of the pole (σ_p, τ_p) is expressed in terms of σ and θ as follows.

$$\left.\begin{aligned}\sigma_p&=\sigma-c_u(z)\cos 2\theta\\ \tau_p&=-c_u(z)\sin 2\theta\end{aligned}\right\} \quad \cdots\cdots(13)$$

The partial derivatives of σ_p and τ_p with respect to s_i $(i=1, 2)$ and their substitution into Eqs. (12·a) and (12·b) yield

$$\left.\begin{aligned}&\cos\beta_2\frac{\partial\sigma_p}{\partial s_1}+\sin\beta_2\frac{\partial\tau_p}{\partial s_1}\\&\quad=\gamma\cos\beta_1\cos\beta_2-\sec\beta_1\frac{\partial c_u(z)}{\partial s_1}\\&\cos\beta_1\frac{\partial\sigma_p}{\partial s_2}+\sin\beta_1\frac{\partial\tau_p}{\partial s_2}\\&\quad=\gamma\cos\beta_1\cos\beta_2-\sec\beta_2\frac{\partial c_u(z)}{\partial s_2}\end{aligned}\right\}\quad\cdots\cdots(14)$$

For the case of normally consolidated clays in which $c_u(z)$ varies linearly with depth,

$$c_u(z)=c_0+\rho z \quad\cdots\cdots(15)$$

Then the fundamental equations for the pole trails become

$$\left.\begin{aligned}&\cos\beta_2\frac{\partial\sigma_p}{\partial s_1}+\sin\beta_2\frac{\partial\tau_p}{\partial s_1}=\gamma\cos\beta_1\cos\beta_2-\rho\\&\cos\beta_1\frac{\partial\sigma_p}{\partial s_2}+\sin\beta_1\frac{\partial\tau_p}{\partial s_2}=\gamma\cos\beta_1\cos\beta_2-\rho\end{aligned}\right\}$$
$$\cdots\cdots(16)$$

Substituting Eq. (10) into Eq. (16), the following two difference equations are obtained:

$$\left.\begin{aligned}(\Delta\tau_p)_{s1}&=\tan\beta_1(\Delta\sigma_p)_{s1}-\gamma\cos\beta_2\Delta s_1\\&\quad+\rho\sec\beta_1\Delta s_1\\(\Delta\tau_p)_{s2}&=\tan\beta_2(\Delta\sigma_p)_{s2}+\gamma\cos\beta_1\Delta s_2\\&\quad-\rho\sec\beta_2\Delta s_2\end{aligned}\right\}\quad\cdots(17)$$

Where the second and the third terms are representing the presence of the unit weight of soil, γ and the rate of increase in strength of soil with depth, ρ respectively. It should be noticed that the rate of increase of cohesion with depth in this Eq. (17) plays the same role as density in the case of the bearing capacity of homogeneous cohesive soils.

Although only the cohesive material $(\phi=0)$ has been treated so far, the graphical solution of plastic equilibrium which took into account the influence of the unit weight for the homogeneous ground $(\rho=0)$ with the internal friction ϕ has been studied by de Josselin de Jong.[7]

(3) Procedures for the Pole Trail Method

Details on the fundamental procedures for the pole trail method are described elsewhere.[4)~6)] Here the method with the unit weight of soil, γ and the rate of strength increase, ρ is to be explained, based on Eq. (17). The stress condition in a soil of plastic equilibrium at point A in **Fig. 4** (a) is represented on the Mohr diagram of **Fig. 4** (b), the difference equation, Eq. (17),

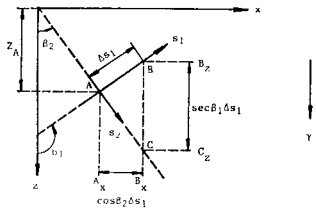

Fig. 4 (a) Physical Space : Construction of Slip Lines.

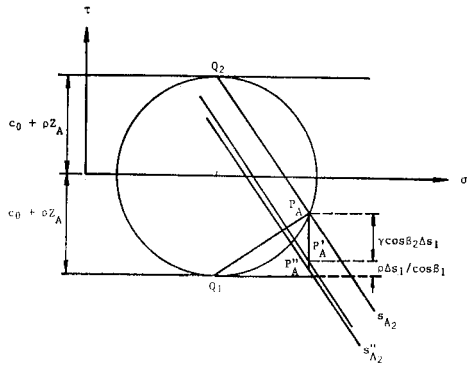

Fig. 4 (b) Stress Space : Construction of Poles.

can be employed to compute the increments $(\Delta\tau_p)_{s1}$ and $(\Delta\sigma_p)_{s1}$ when the position changes from A to B along a slip line s_1 (*i.e.*, Δs_1) in **Fig. 4** (a). The pole P_B in the stress space corresponding to the point B in the physical space is determined to lie on the line s_{A_2}'' as shown in **Fig. 4** (b). In other words, set a point $P_{A'}$ which shifts by $\gamma\cos\beta_2\Delta s_1$ from the point P_A (in this case, in the direction of the body force, *i.e.* in the opposite direction of τ axis in stress space)* and furthermore set a point $P_{A''}$ shifting by ρ sec $\beta_1\Delta s_1$ from $P_{A'}$. And then the point P_B is found on a line s_{A_2}'' which passes through the point $P_{A''}$ and is parallel to the slip lines s_2.

The distance between the line s_{A_2}'' and the line s_{A_2} in the direction parallel to the τ-axis of the stress space is equal to the sum of the second and third terms of the right hand side of Eq. (17). The intersection of the slip line $(s_2)_A$ and the line parallel to the Z-axis of the physical space through a point B yields a point C. Then the meanings of the second and third terms are shown geometrically as follows:

* The shift direction is determined from the directions of s_1, s_2 and from the angles of β_1, β_2. Details should be refered to Reference 5.

a) the second term

The second term of the right hand side of Eq. (17), $\gamma \cos\beta_2 \Delta s_1$ is equal to the unit weight of the soil times the horizontal projection of the distance $\overline{AB}$ on the X-axis, $\overline{A_xB_x}$ in the physical space of **Fig. 4** (a), *i.e.*:

$$\overline{A_xB_x}=\cos\beta_2\Delta s_1$$

b) the third term

The third term, $\rho \sec\beta_1 \Delta s_1$ is equal to the rate of strength increase with depth times the vertical intercept $\overline{B_zC_z}$ from the geometric property, *i.e.*:

$$\overline{B_zC_z}=\sec\beta_1\Delta s_1$$

as shown in **Fig. 4** (a).

Similar procedure can be employed along the alternate slip line s_2 and the stress state of the desired point may be obtained. In the case of the soil without weight and without any rate of strength increase with depth, the pole trail method is easily performed without taking into account the second and third terms of Eq. (17).

The stress conditions at points A, B and C shown in **Fig. 5** (a) are represented in the stress space of **Fig. 5** (b). In general, the position of the pole P_C corresponding to the point C is unknown and must be found from the known poles, P_A and P_B. Let the two slip lines through points A and B define the lines s_{A_1}, s_{A_2}, s_{B_1}, s_{B_2}.

Just as the intersection of the two slip lines, s_{A_1} and s_{B_2} through points A and B in **Fig. 5** (a) yields point C by using the pole trail method along each slip line, the intersection of the lines $s_{A'_2}$ and $s_{B'_1}$ which are parallel to the alternate slip lines in the stress space (**Fig. 5** (b)) gives the position of the pole of point C, P_C. When the position of the pole P_C is known, the Mohr circle for the point C can be drawn tangential to the failure line defined by Eq. (15), with its center on the σ-axis and passing through point P_C. Once the stress circle for the point C is drawn, the directions of the slip lines through the point C in the physical space are given by the lines through the pole of point C, P_C and the contact points of the Mohr circle for C and the failure line.

The points C and P_C obtained by the procedure described above are only of the first order approximation and then the correct position of the pole, P_C^c must be determined by trial and error, repeating the same procedure: that is, at first in stress space the directions of conjugate slip lines at the point C is determined from **Fig. 5** (b) and then slip lines s_{A_1} and s_{B_2} in physical space are corrected by bending at each middle point of AC and BC, which become parallel to the new slip lines at C. The intersection of these corrected slip lines of s_{A_1} and s_{B_2} is to be a better point C'. The better position of the pole, P'_C, is constructed in stress space by correcting *i.e.*, bending the conjugate slip lines $s_{A_2'}$ and $s_{B_1'}$, which should be parallel to the corrected slip lines in physical space. The best positions for C and P_C will be obtained by a few trials, and then these are considered to be the correct ones. These points C^c and P_C^c become the basis for further construction of the slip line net.

In the stress space of **Fig. 5** (b), the pole for each point along a slip line is obtained as a locus of the original starting pole formed as the Mohr circle at the starting point rolls along a failure line without slipping and at the same time expands or contracts to maintain the condition of tangency with the failure line. This locus of the original starting pole may be thought of as a generalized form of cycloid.

In the special case where the material without weight possesses a constant cohesive strength and the yield line is parallel to the σ-axis in the stress space, it will be noted the locus of the pole is a cycloid, without expansion or contraction.

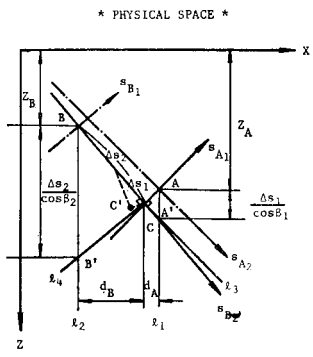

Fig. 5 (a) Physical Space.

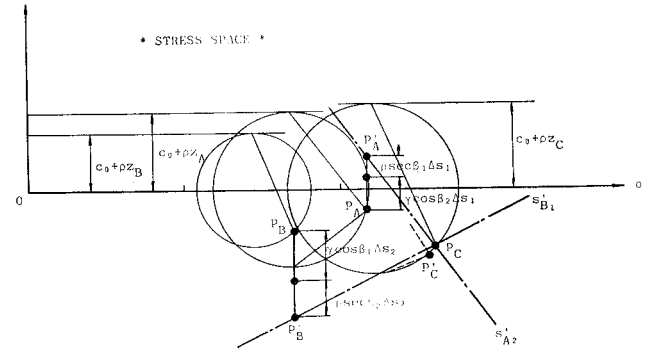

Fig. 5 (b) Stress Space.

(4) Bearing Capacity of Cohesive Soil Deposit

When the shear strength of a saturated soil is expressed in a total stress, the cohesive strength c_u is a function of water content or void ratio which is dependent upon the effective stress. Therefore for soil which deposited under the gravity force, the own weight of the soil causes a decrease in void ratio with depth. This decrease in void ratio often causes an approximately linear increase in strength with depth. Practically, the strength of the cohesive soil may be allowed to express

$$c_u=\rho z \quad \text{(Normally consolidated)} \cdots(18\cdot a)$$

$$c_u=c_0+\rho z \quad \text{(Overconsolidated)} \cdots\cdots(18\cdot b)$$

In other words, the assumption that c_u is constant throughout the soil ground has the same meaning that the void ratio or water content is constant. However, since the effective stress due to the own weight of soil increases with depth, the conclusion that the consolidation is not proceeded as the depth increases must consequently be obtained, but clearly this is not realistic.

For a structure with a normal size, the bottom of the slip line is close to the ground surface and there is no need to consider the rate of strength increase with depth. On the other hand, for a huge structure the assumption that c_u is constant may not be allowed because of great influence on the wide range in the ground. Therefore the bearing capacities for both cases should be compared and their differences must be investigated.

Before an example calculation, let us now examine what the rate of strength increase with depth, ρ is. It is well-known that in natural soil deposit the cohesion c_u is linearly dependent upon the effective stress, p and the ratio c_u/p is the rate of strength increase due to consolidation, which is function of plasticity index, PI. For a normally consolidated soil where the ground water level coincides with the ground surface, Eq. (18) is modified to:

$$\rho=c_u/z=\frac{c_u}{\gamma' z}\gamma'=\frac{c_u}{p}\gamma' \quad \cdots\cdots(19)$$

$$\rho/\gamma'=c_u/p \quad \cdots\cdots(19)'$$

Therefore, the ratio c_u/p is related to ρ by Eq. (19) or Eq. (19'). In the following example, the values of $c_u/p=0.3$ and $\gamma'=0.9$ t/m^3 are adopted for a usual cohesive soil medium and then ρ is calculated to be 0.27 t/m^3. **Fig. 6** (a) shows slip lines in the physical space and the trajectries of the poles in the stress space are shown in **Fig.** 6 (b).

For a homogeneous soil there exists a quadrant sector plastic region below the point O (the edge of footing) and the slip lines make a regular mesh in the active and passive regions. On the contrary, for an inhomogeneous ground, the slip lines of the s_2 family densely gather below the point O and the slip lines of the s_1 family become flat. Then the trajectries of the poles as shown in **Fig. 6** (b) roll up to the left and finally reach the σ-axis such as 3D→3f→3g→3B in the figure.

The distribution of vertical stress (major principal stress) along the bottom of the foundation at plastic equilibrium is shown in **Fig. 6** (c)

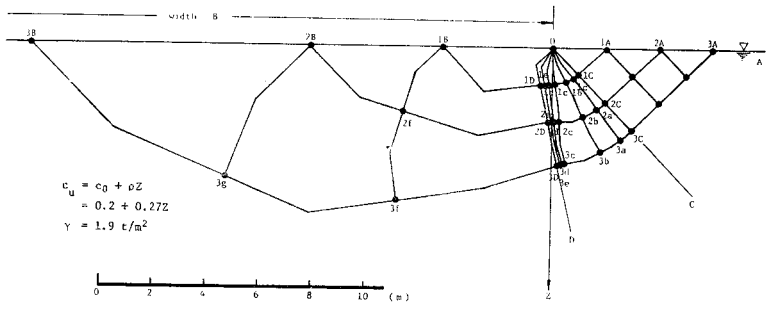

Fig. 6 (a) Physical Space (Trajectories of Slip Lines).

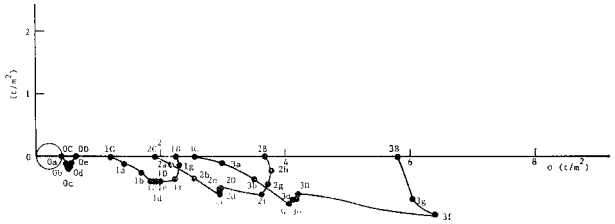

Fig. 6 (b) Stress Space (Trajectories of Poles).

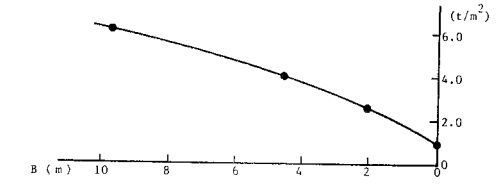

Fig. 6 (c) Distribution of Major Principal Stress along Foundation Base.

Table 1 Comparison between Bearing Capacities Calculated by Conventional Methods and Graphical Pole Trail Method.

Method \ B (m)	2	4	6	8	10
(1) Graphical Solution of Plastic Equilibrium	1.87	2.54	3.12	3.63	4.08
(2) Terzaghi or Prandtl $q_d=5.14c_u$	1.95	2.89	3.80	4.73	5.65
(3) $\phi=0$-Slip Circle Method	2.08	2.92	3.70	4.46	5.18

(t/m²)

as a result of computation and the value of the limit bearing capacity, q_d is listed in **Table** 1 as the Method (1). The Method (2) is calculated from Eq. (4) by Prandtl and the average value of cohesion c_u used in the computation is the value of a point at the depth of 1/3 of the foundation width.[8] The Method (3) is the graphical solution by $\phi=0$-slip circle analysis in which the rate of strength increase with depth is taken into account.

From **Table** 1, it is known that the value of bearing capacity by the pole trail method is smaller than by other methods, with the increase of the foundation width. If this pole trail method gives the almost exact solution, the inhomogeneity of the ground must be considered as a very important factor which influences on the reduction of the bearing capacity.

4. APPLICATION OF GRAPHICAL SOLUTION TO WEATHERED ROCK MASS

(1) Introduction

Generally speaking, the effect of cohesive strength of the ground on the bearing capacity of foundation is very large. It is often seen that there is a considerable difference between the results of bearing capacity without cohesion and a small amount of cohesion, *e.g.* $c=0.1$ t/m² for a soil or rock material whose cohesive strength is nearly equal to zero. This effect is usually great when the length of the slip face at plastic failure is large, because the cohesive strength is exerted uniformly along the slip surface. On the contrary, the resistance by internal friction is exerted depending upon the magnitude of normal stress on the slip surface.

The geologic material whose strength is mainly governed by a cohesion is a cohesive soil or clay and the behavior of weathered granite resembles that of sand whose cohesive strength is negligible. However, the apparent cohesive strength for such material is often noticed due to the nonlinear failure envelope and the history of overconsolidation.

The history of overconsolidation can be detected by the shape of stress paths in shearing. **Fig. 7** shows the schematic diagram of stress paths when the triaxial compression test (CU-test) is performed for a geologic material which was taken from a point subjected to a larger load in the past than the present surcharge. When the effective confining pressure at the beginning of the test is greater than the preconsolidation pressure of the specimen (normally consolidated state), the effective stress path is always in the left side of the total stress path (straight line with the slope of 3 to 1) and the positive pore pressure is induced. On the other hand, when the effective confining pressure is smaller than the preconsolidation pressure (overconsolidated state), the stress path initially rises vertically or to the right and the pore pressure gradually decreases. In some cases, it may cross the total stress path and the induced pore pressure may become negative. From these facts and the shape of the failure envelope in **Fig. 7**, the history of overconsolidation of a geologic material can be estimated. As a matter of fact, the region of overconsolidation is not easily found from the failure envelope because the change of slope of the failure curve is not clearly shown in Mohr diagram written in effective stresses. Then the former method, use of the effective stress path, is better to understand the history of overconsolidation.

The most frequently used failure criterion for geologic materials is one by Mohr, which is schematically shown in **Fig. 8**. The Mohr failure

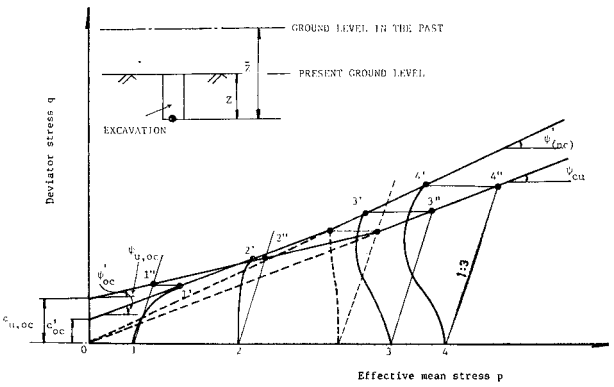

Fig. 7 Stress Paths for a Soil Element in the Ground.

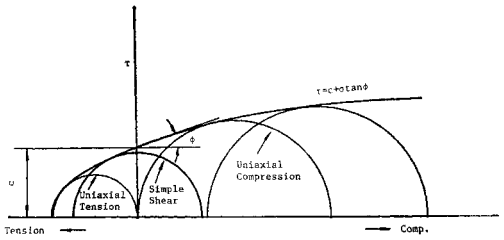

Fig. 8 Nonlinear Mohr Failure Envelope.

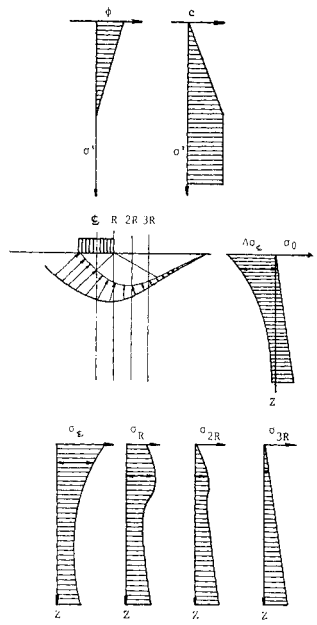

Fig. 9 Distribution of Stress at Slip Failure.

criterion is generally written as:

$$\tau = f(\sigma')$$

Coulomb wrote this equation as

$$\tau = c' + \sigma' \tan\phi$$

This linear type of the failure criterion is called as the Mohr-Coulomb failure criterion, which is usually applied to soils.

It is a well-known fact that the geologic materials become ductile under a relatively high confining pressure and they behave like a cohesive material rather than a frictional one in a such circumstance, and their failure curves are bent and gradually become flat. Therefore the shear strength constants (c', ϕ') of these geologic material are dependent upon the effective stress and can not be determined uniquely.

As is known from above statements, the conventional equations for bearing capacity can not be applied to the problem of the ground in which the strength parameters are depending upon the effective stress, because in such ground not only the shear resistance is nonuniform along the slip failure surface but also the strength parameters are a function of the position of a soil element as shown in **Fig. 9**. It is seen that the normal stresses acting on the slip surface are different at each point in the ground and therefore the strength parameters must be selected for each point in order to estimate the correct solution of the bearing capacity.

(2) Strength Characteristics of Weathered Granite[9]

a) Rock Sample

The rock sample tested in the laboratory is the Hiroshima type weathered granite which is in D_L class. This sample is heavily weathered and its mineral ingredients are altered to clay. Since cracks and discontinuities are not found in the specimen whose physical properties are shown in **Table 2**, there is essentially no difference between the property of the sample and that of the rock mass. In order to investigate the strength characteristics of such weathered rock, the laboratory and in-situ tests were carried out.

Table 2 Physical Properties of Weathered Granite.

Sample	w (%)	e	γ (g/cm³)	γ_d (g/cm³)	G_s	S_r (%)
Site 1	17.2	0.50	1.968	1.682		
Site 2	22.6	0.650	1.921	1.571		
Site 3	17.0	0.49	1.962	1.676	2.60	90.0
Site 4	16.3	0.47	1.953	1.680		
Average	18.2	0.53	1.948	1.651		

w: Water Content e: Void Ratio
γ: Mass Density γ_d: Dry Density
G_s: Specific Gravity of Solid S_r: Degree of Saturation

b) Triaxial Compression Test

The triaxial compression test was performed in a consolidated-undrained condition with a constant confining pressure and a constant strain rate of about 0.045%/min. The pore pressure induced during the test was continuously measured. The Mohr circle and a failure envelope for the sample at the instant when the induced pore pressure is maximum is shown in **Fig. 10**. It is known from **Fig. 10** that the failure envelope of this sample is not linear.

While several methods have been known to determine the strength of the intact rock, the definite way of strength determination of a soft rock such as weathered granite, which shows a

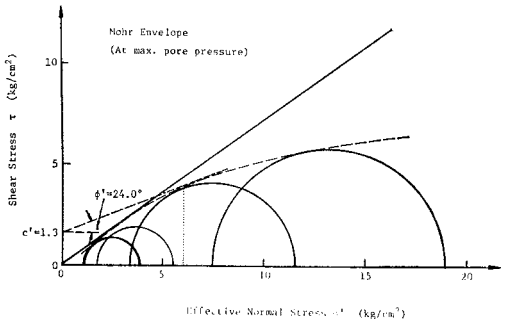

Fig. 10 Mohr Circles for Weathered Granite.

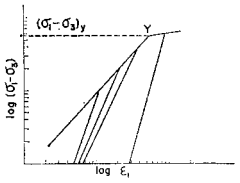

Fig. 11 Diagramatic Representation of Stress-Strain Curve Plotted in Log-Log Scale.

non-linear stress-strain relation over the all stress ranges, is not established yet. Therefore, we now estimate the strength of soft rock by the following two methods. The first method is that if a stress-strain curve is plotted in the log-log scale, it is approximated by two lines broken at the yield point (Y point) as shown in **Fig. 11**. The second method is that the turning point of volume change or induced pore pressure (M point) is determined as a yield point.

In an undrained triaxial test, the induced pore pressure increases with the axial stress and shows a peak point (M point), after which it tends to decrease when the deformation continues. This means that, in a drained test, the volume of the rock specimen starts to expand at this M point. This feature of the material is called dilatancy and M point can be considered to be a special point for the geologic material, a drastic change of the structure in the material.

Fig. 12, which is redrawn from the result of **Fig. 10**, shows the yield lines for both Y and M points, and the effective stress paths during the shearing of the specimens. Under the consolidation pressures of 1–2 kg/cm², the stress paths rise almost vertically and arrive at the failure line, curving to the right just like over-consolidated clay.

The stress paths under the consolidation pressures of greater than 3 kg/cm² are similar to normally consolidated clay, and the paths turn to the left with an increase of the induced pore pressure and reach the failure line. However, the paths, after arriving at the failure line, change their direction with a decrease of the pore pressure due to dilatancy, while the strength of the specimen continued to increase. The ▲ marks in **Fig. 12** indicate the stress paths for the triaxial creep test with the same sample. **Table 3** shows the strength parameters determined by Y and M points for the weathered granite.

Table 3 Strength Parameters for Weathered Granite.

	c'_{cu}	ϕ'_{cu}	c_u/σ_c'
Y	0	21.6°	0.33
M	0	35.3°	0.48

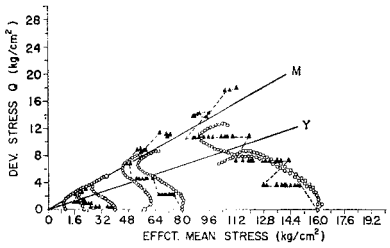

Fig. 12 Stress Paths of Weathered Granite.

c) In-Situ Test

In order to obtain directly the engineering properties of rock mass, in-situ direct shear and plate bearing tests were conducted in a vertical shaft which was excavated down to the depth of 10 m. The laboratory specimens were taken from the bottom of the shaft.

The in-situ direct shear test was done by excavating a rock block in the shaft. For a very

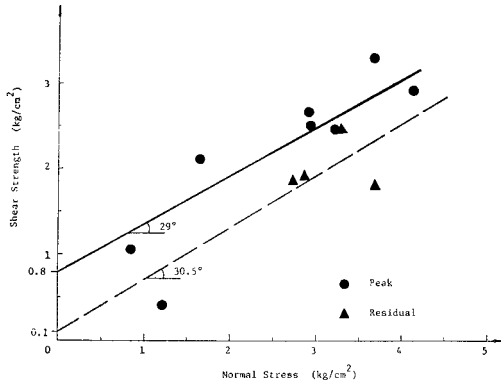

Fig. 13 Results of In-Situ Direct Shear Test.

fragile rock block, the ring shear test was performed by confining the rock block with steel pipes. The results of the tests are shown in **Fig. 13**. Although there is a scattering of the results, the average strength parameters for peak values of shearing stress may be $c=8$ t/m^2 and $\phi=29°$. The parameters for residual strength are $c=1$ t/m^2 and $\phi=30.5°$.

The plate bearing tests with a diameter of 40 cm indicated that the yielding strength and the bearing capacity of the rock mass are in the range of 60–160 t/m^2 and 120–160 t/m^2, respectively.

d) Bearing Capacity of Weathered Rock Mass[10]

By means of strength parameters determined by triaxial tests, the graphical solution is applied to the problem of bearing capacity of weathered rock mass of granite ($\phi=0$-analysis). The ground condition used is shown in **Fig. 14**. The material constants are obtained from the triaxial consolidated undrained test results as shown in **Fig. 15**, in which the point of strength is taken to be at maximum pore pressure (point M) because we now consider the short-term stability analysis only.[9] **Fig. 16** (a) is the physical space and **Fig. 16** (b) is the corresponding stress space for a foundation on the weathered rock mass.

Being subjected to vertical loading, the rock under OB and OA is in a state of plastic equilibrium. At any point along the base OB, σ_z and σ_x are a major and a minor principal stress respectively, and the rock mass immediately under the footing is in the active state. Therefore along the surface OB, θ is equal to zero and the slopes of the two families of slip lines (s_1 and s_2 lines) with respect to the Z-axis are $+\pi/4$ and $-\pi/4$, respectively. In the region immediately below the surface along OA, the passive Rankine state, the constant normal stress (*i.e.*, surcharge) at the boundary is a minor principal stress and the horizontal stress σ_x is a major. In this passive region, $\theta=\pi/2$ and the slopes of the two slip lines below the surface are $3\pi/4$ and $\pi/4$, respectively. From the boundary condition on OA, the stresses in the region AOC are determined, taking into account the unit weight of soil and the rate of strength increase.

The point O is a singular point in the region, representative of the stress discontinuity, and exists at the edge of the foundation and also all slip lines of the s_2 family between the lines OC and OD pass through the point O. The requirement that the two families of slip lines intersect each other at the angle of $\pi/2$ means that the slip lines of the s_1 family are curved in the region COD.

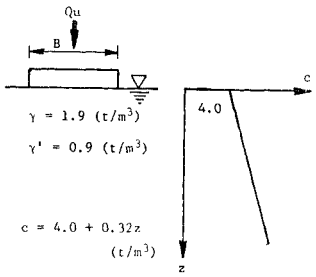

Fig. 14 Ground Condition for Weathered Rock Mass.

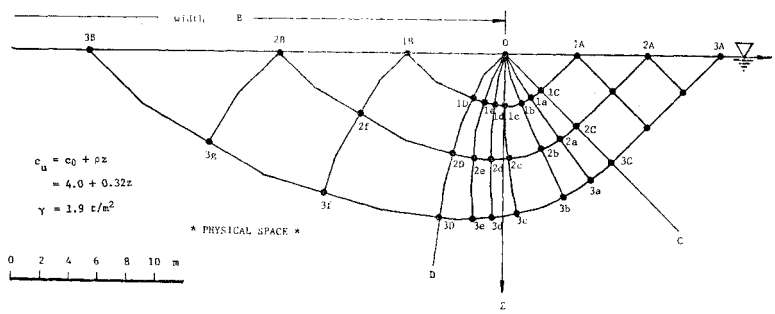

Fig. 16 (a) Physical Space.

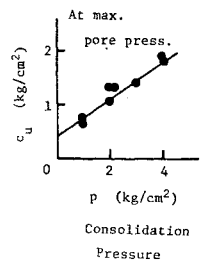

Fig. 15 Relationship between the Undrained Shear Strength and Consolidation Pressure.

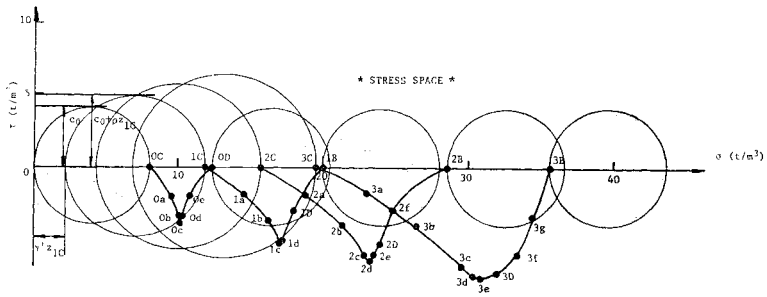

Fig. 16 (b) Stress Space.

Starting from the vicinity of the point O, the first step to construct a slip line net is to divide the angle COD into an adequate number of equal angle. Since the point O is close enough to the surface to neglect the weight and strength increase of soil, the locus of the pole along a slip line of the s_1 family in the vicinity of the point O is easily obtained according to the pole trail method and the result is shown in **Fig. 16** (b) as the trace of the pole from OC to OD through Oc.

Following the straight-line portion in the region AOC and based on the locus of the pole obtained as stated above, a slip line of the s_1 family is extended through a point nC ($n=1, 2, \ldots$) to intersect the s_2 slip lines Oa at a point na, or at a point nb, . . . , along the curve nCnD in the area COD to the point nD, and finally the s_2 lines reach the negative X-axis in a point nB along another curve nDnB.

By suitable choice of the point nA, the loaded portion OnB (the width of a foundation) is extended to the negative X-axis direction. Repetition of this procedure results in the determination of the slip-line field with a desired degree of approximation depending upon the mesh refinement in the semi-infinite medium. **Fig. 17** shows the distribution of the major principal stresses calculated by the above method. The bearing capacity determined by the pole trail method was compared with the ones by the conventional methods in **Table 4**. It shows that the conventional methods overestimate the bearing capacity 10–20% greater than the graphical solution of the pole trail method. From the distribution of the major normal principal stresses in **Fig. 17**, it is noticed that the larger the width of foundation is, the greater the discrepancy between Method (1) and Method (2) becomes, and Method (3) gives the most overestimated values of bearing capacity as is shown in **Table 1**.

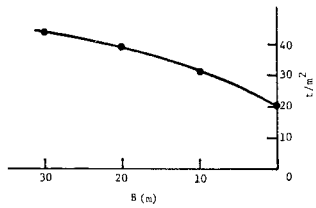

Fig. 17 Distribution of Major Principal Stress along Foundation Base.

Table 4 Comparison between Bearing Capacities Calculated by Conventional Methods and Graphical Pole Trial Method.

B (m)	10	20	30
(1) Graphical Solution of Plastic Equilibrium	26.0	30.9	34.7
(2) Terzaghi $q_d=5.14c_u$	26.1	31.5	37.0
(3) ϕ=0-Slip Circle Analysis	29.2	35.2	40.0

t/m²

The bearing capacity determined by the field tests is extremely greater than that by the graphical solution. This is partly because the surcharge is not taken into account in this graphical solution. Another reason is that the graphical solution described in this paper can only be applied to the problem of bearing capacity of cohesive soil or rock ($\phi=0$) which is inhomogeneous in the vertical direction only, whereas the actual ground may have different values of ϕ unless the load is applied instantaneously. Therefore an improved graphical method will be required which can be applied to the problem of bearing capacity of the ground in which cohesion increases with depth and the angle of internal friction, ϕ is not zero.

5. CONCLUSION

The graphical solution of the pole trail method based on the theory of plasticity was proposed to obtain the bearing capacity of a foundation on inhomogeneous ground whose strength is a function of the depth from the ground surface and the method was applied to the problem of the foundation on the weathered rock mass. The conclusions obtained in this study are as follows.

(1) The graphical solution which does not take into account the soil weight and any rate of increase in strength with depth seriously overestimates the bearing capacity of inhomogeneous ground.

(2) The graphical solution developed in this paper can be applied to all sorts of problems of bearing capacity of cohesive material ($\phi=0$) which is inhomogeneous in the vertical direction only. In this solution, it was found that the rate of increase of cohesion with depth, ρ plays a same role as the unit weight, γ.

(3) The use of slip circle analysis and Terzaghi's equation for the problems where inhomogeneity of the ground is dominant should be viewed critically, since it postulates a possible mode of moment without evaluation of complete stress distribution.

(4) The bearing capacity of the weathered rock mass of granite was determined by the graphical solution of the pole trail method by

using the data from the laboratory experiments. The bearing capacity of the foundation is found to be dependent markedly upon the width of the foundation and the conventional methods overestimate the bearing capacity 10–20% greater than the pole trail method.

REFERENCES

1) Davis, E. H. and Booker, J. R.: The Effect of Increasing Strength with Depth on the Bearing Capacity of Clay, Geotechnique 23, No. 4, pp. 551–563, 1973.
2) Davis, E. H. and Booker, J. R.: Application of Plasticity Theory to Foundations, Proc. of the General Session of the Symposium Held at the Univ. of New South Wales, Australia, 1975.
3) Spencer, A. J. M.: Perturbation Methods in Plasticity-I. Plane Strain of Non-homogeneous Plastic Solids, J. Mech. Phys. Solids, Vol. 9, pp. 279–288, 1961.
4) Scott, R. F.: Principles of Soil Mechanics, Appendix C, Addison & Wiley, 1963.
5) Komada, K.: The Principle of Graphical Method for the Stresses of Soil in the State of Plastic Equilibrium, The Report of Public Works Research Institute, No. 237, Ministry of Construction, 1967.
6) Komada, K.: The Representation of Mohr's Stress Circle and Application, No. 2, Soils and Foundations, Vol. 21, No. 4, pp. 71–74, 1973.
7) De Josselin de Jong: Statics and Kinematics in the Failable Zone of a Granular Material, Waltman, Delft, 1959.
8) Raymond, G. P.: The Bearing Capacity of Large Footings and Embankments on Clays, Geotechnique 17, No. 1, pp. 1–10, 1967.
9) Akai, K., Adachi, T., Yamamoto, K. and Ohnishi, Y.: Strength Characteristics of Weathered Granite, Memoirs of Faculty of Engineering, Kyoto Univ., Vol. 38, Part 4, 1976.
10) Akai, K., Ohnishi, Y. and Mizobe, H.: Bearing Capacity of Weathered Rock Mass, Proc. of 5th Symp. of Rock Mechanics in Japan, 1977.

(*Received April 22, 1977*)